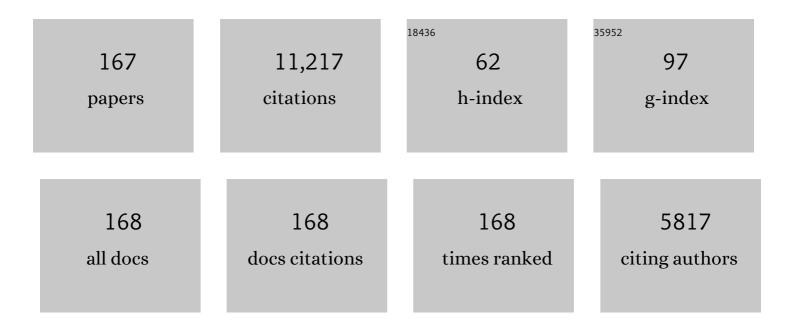
List of Publications by Year in descending order

Source: https://exaly.com/author-pdf/369535/publications.pdf Version: 2024-02-01



VUE DENC

#	Article	IF	CITATIONS
1	Cerium-tungsten oxides supported on activated red mud for the selective catalytic reduction of NO. Green Energy and Environment, 2023, 8, 173-182.	4.7	4
2	Electronic structure tailoring of Al3+- and Ta5+-doped CeO2 for the synergistic removal of NO and chlorinated organics. Applied Catalysis B: Environmental, 2022, 304, 120939.	10.8	42
3	Carbon/chlorinate deposition on MnOx-CeO2 catalyst in chlorobenzene combustion: The effect of SCR flue gas. Chemical Engineering Journal, 2022, 433, 133552.	6.6	28
4	Revealing the Synergistic Deactivation Mechanism of Hydrothermal Aging and SO ₂ Poisoning on Cu/SSZ-13 under SCR Condition. Environmental Science & Technology, 2022, 56, 1917-1926.	4.6	34
5	Improvement of Al2O3 on the multi-pollutant control performance of NOx and chlorobenzene in vanadia-based catalysts. Chemosphere, 2022, 289, 133156.	4.2	13
6	Insights into the binding manners of an Fe doped MOF-808 in high-performance adsorption: a case of antimony adsorption. Environmental Science: Nano, 2022, 9, 254-264.	2.2	10
7	Identification of Intrinsic Active Sites for the Selective Catalytic Reduction of Nitric Oxide on Metal-Free Carbon Catalysts via Selective Passivation. ACS Catalysis, 2022, 12, 1024-1030.	5.5	17
8	Synergistic Effects of a CeO ₂ /SmMn ₂ O ₅ –H Diesel Oxidation Catalyst Induced by Acid-Selective Dissolution Drive the Catalytic Oxidation Reaction. ACS Applied Materials & Interfaces, 2022, 14, 2860-2870.	4.0	8
9	Intra-crystalline mesoporous zeolite encapsulation-derived thermally robust metal nanocatalyst in deep oxidation of light alkanes. Nature Communications, 2022, 13, 295.	5.8	54
10	New insight on electroreduction of nitrate to ammonia driven by oxygen vacancies-induced strong interface interactions. Journal of Catalysis, 2022, 406, 39-47.	3.1	29
11	Activating Surface Lattice Oxygen of a Cu/Zn _{1<i>–x</i>} Cu _{<i>x</i>} O Catalyst through Interface Interactions for CO Oxidation. ACS Applied Materials & Interfaces, 2022, 14, 9882-9890.	4.0	13
12	Dual Active Centers Bridged by Oxygen Vacancies of Ruthenium Singleâ€Atom Hybrids Supported on Molybdenum Oxide for Photocatalytic Ammonia Synthesis. Angewandte Chemie, 2022, 134, .	1.6	8
13	Dual Active Centers Bridged by Oxygen Vacancies of Ruthenium Singleâ€Atom Hybrids Supported on Molybdenum Oxide for Photocatalytic Ammonia Synthesis. Angewandte Chemie - International Edition, 2022, 61, .	7.2	45
14	Like Cures like: Detoxification Effect between Alkali Metals and Sulfur over the V ₂ O ₅ /TiO ₂ deNO _{<i>x</i>} Catalyst. Environmental Science & Technology, 2022, 56, 3739-3747.	4.6	38
15	Metal–Support Interactions within a Dual-Site Pd/YMn ₂ O ₅ Catalyst during CH ₄ Combustion. ACS Catalysis, 2022, 12, 4430-4439.	5.5	16
16	Interaction Mechanism for Simultaneous Elimination of Nitrogen Oxides and Toluene over the Bifunctional CeO ₂ –TiO ₂ Mixed Oxide Catalyst. Environmental Science & Technology, 2022, 56, 4467-4476.	4.6	47
17	Efficient Electron Transfer by Plasmonic Silver in SrTiO ₃ for Low-Concentration Photocatalytic NO Oxidation. Environmental Science & Technology, 2022, 56, 3604-3612.	4.6	29
18	Efficient Electrochemical Nitrate Reduction to Ammonia with Copperâ€Supported Rhodium Cluster and Singleâ€Atom Catalysts. Angewandte Chemie - International Edition, 2022, 61, .	7.2	170

#	Article	IF	CITATIONS
19	Efficient Electrochemical Nitrate Reduction to Ammonia with Copper‣upported Rhodium Cluster and Singleâ€Atom Catalysts. Angewandte Chemie, 2022, 134, .	1.6	28
20	Selective Catalytic Reduction of NO _{<i>x</i>} with NH ₃ over Cu/SSZ-13: Elucidating Dynamics of Cu Active Sites with In Situ UV–Vis Spectroscopy and DFT Calculations. Journal of Physical Chemistry C, 2022, 126, 8720-8733.	1.5	20
21	Photothermal Synergistic Effect of Pt ₁ /CuO-CeO ₂ Single-Atom Catalysts Significantly Improving Toluene Removal. Environmental Science & Technology, 2022, 56, 8722-8732.	4.6	52
22	Hierarchically devising NiFeO H catalyst with surface Fe active sites for efficient oxygen evolution reaction. Catalysis Today, 2021, 364, 140-147.	2.2	14
23	Theory and practice of metal oxide catalyst design for the selective catalytic reduction of NO with NH3. Catalysis Today, 2021, 376, 292-301.	2.2	71
24	Activity improvement of acid treatment on LaFeO3 catalyst for CO oxidation. Catalysis Today, 2021, 376, 205-210.	2.2	21
25	Facile synthesis λâ€MnO2 spinel for highly effective catalytic oxidation of benzene. Chemical Engineering Journal, 2021, 421, 127828.	6.6	21
26	Simultaneous removal of NOx and chlorobenzene on V2O5/TiO2 granular catalyst: Kinetic study and performance prediction. Frontiers of Environmental Science and Engineering, 2021, 15, 1.	3.3	26
27	Sacrificial carbon strategy for facile fabrication of highly-dispersed cobalt-silicon nanocomposites: Insight into its performance on the CO and CH4 oxidation. Journal of Cleaner Production, 2021, 278, 123920.	4.6	6
28	Synthesis of α–MnO2–like rod catalyst using YMn2O5 A–site sacrificial strategy for efficient benzene oxidation. Journal of Hazardous Materials, 2021, 403, 123811.	6.5	32
29	Surface In Situ Doping Modification over Mn ₂ O ₃ for Toluene and Propene Catalytic Oxidation: The Effect of Isolated Cu ^{Î+} Insertion into the Mezzanine of Surface MnO ₂ Cladding. ACS Applied Materials & Interfaces, 2021, 13, 2753-2764.	4.0	53
30	Predicting the adsorption of organic pollutants on boron nitride nanosheets <i>via in silico</i> techniques: DFT computations and QSAR modeling. Environmental Science: Nano, 2021, 8, 795-805.	2.2	13
31	Multipollutant Control (MPC) of Flue Gas from Stationary Sources Using SCR Technology: A Critical Review. Environmental Science & Technology, 2021, 55, 2743-2766.	4.6	117
32	Superior Oxidative Dehydrogenation Performance toward NH ₃ Determines the Excellent Low-Temperature NH ₃ -SCR Activity of Mn-Based Catalysts. Environmental Science & Technology, 2021, 55, 6995-7003.	4.6	83
33	Multi-pollutant control (MPC) of NO and chlorobenzene from industrial furnaces using a vanadia-based SCR catalyst. Applied Catalysis B: Environmental, 2021, 285, 119835.	10.8	54
34	Fabrication of Nanohybrid Spinel@CuO Catalysts for Propane Oxidation: Modified Spinel and Enhanced Activity by Temperature-Dependent Acid Sites. ACS Applied Materials & Interfaces, 2021, 13, 27106-27118.	4.0	30
35	New Insights on Competitive Adsorption of NO/SO ₂ on TiO ₂ Anatase for Photocatalytic NO Oxidation. Environmental Science & Technology, 2021, 55, 9285-9292.	4.6	24
36	Boosting nitrous oxide direct decomposition performance based on samarium doping effects. Chemical Engineering Journal, 2021, 414, 128643.	6.6	30

#	Article	IF	CITATIONS
37	Impact of NOx and NH3 addition on toluene oxidation over MnOx-CeO2 catalyst. Journal of Hazardous Materials, 2021, 416, 125939.	6.5	37
38	Balance of activation and ring-breaking for toluene oxidation over CuO-MnO bimetallic oxides. Journal of Hazardous Materials, 2021, 415, 125637.	6.5	49
39	Boosting the Catalytic Performance of CeO ₂ in Toluene Combustion via the Ce–Ce Homogeneous Interface. Environmental Science & Technology, 2021, 55, 12630-12639.	4.6	71
40	Mercury speciation and size-specific distribution in filterable and condensable particulate matter from coal combustion. Science of the Total Environment, 2021, 787, 147597.	3.9	14
41	Inhibition Effect of Phosphorus Poisoning on the Dynamics and Redox of Cu Active Sites in a Cu-SSZ-13 NH ₃ -SCR Catalyst for NO <i>_x</i> Reduction. Environmental Science & Technology, 2021, 55, 12619-12629.	4.6	43
42	Alloying effect-induced electron polarization drives nitrate electroreduction to ammonia. Chem Catalysis, 2021, 1, 1088-1103.	2.9	80
43	Balancing redox and acidic properties for optimizing catalytic performance of SCR catalysts: A case study of nanopolyhedron CeO -supported WO. Journal of Environmental Chemical Engineering, 2021, 9, 105828.	3.3	7
44	A novel Î ³ -like MnO2 catalyst for ozone decomposition in high humidity conditions. Journal of Hazardous Materials, 2021, 420, 126641.	6.5	33
45	Key intermediates from simultaneous removal of NO _{<i>x</i>} and chlorobenzene over a V ₂ O ₅ –WO ₃ /TiO ₂ catalyst: a combined experimental and DFT study. Catalysis Science and Technology, 2021, 11, 7260-7267.	2.1	9
46	Insight into the promotion mechanism of activated carbon on the monolithic honeycomb red mud catalyst for selective catalytic reduction of NOx. Frontiers of Environmental Science and Engineering, 2021, 15, 1.	3.3	14
47	High Selectivity to HCl for the Catalytic Removal of 1,2-Dichloroethane Over RuP/3DOM WO _{<i>x</i>} : Insights into the Effects of P-Doping and H ₂ O Introduction. Environmental Science & Technology, 2021, 55, 14906-14916.	4.6	33
48	Surface Reconstruction of a Mullite-Type Catalyst via Selective Dissolution for NO Oxidation. ACS Catalysis, 2021, 11, 14507-14520.	5.5	27
49	A multiple-active-site Cu/SSZ-13 for NH3-SCO: Influence of Si/Al ratio on the catalytic performance. Catalysis Communications, 2020, 135, 105751.	1.6	40
50	Comparative study of α-, β-, γ- and Β-MnO2 on toluene oxidation: Oxygen vacancies and reaction intermediates. Applied Catalysis B: Environmental, 2020, 260, 118150.	10.8	400
51	A new insight into adsorption state and mechanism of adsorbates in porous materials. Journal of Hazardous Materials, 2020, 382, 121103.	6.5	38
52	The effect of additives and intermediates on vanadia-based catalyst for multi-pollutant control. Catalysis Science and Technology, 2020, 10, 323-326.	2.1	25
53	Core-shell-like structured α-MnO2@CeO2 catalyst for selective catalytic reduction of NO: Promoted activity and SO2 tolerance. Chemical Engineering Journal, 2020, 391, 123473.	6.6	50
54	Modified red mud catalyst for the selective catalytic reduction of nitrogen oxides: Impact mechanism of cerium precursors on surface physicochemical properties. Chemosphere, 2020, 257, 127215.	4.2	25

#	Article	IF	CITATIONS
55	Nb-incorporated Fe (oxy)hydroxide derived from structural transformation for efficient oxygen evolution electrocatalysis. Journal of Materials Chemistry A, 2020, 8, 24598-24607.	5.2	18
56	Nature of active Fe species and reaction mechanism over high-efficiency Fe/CHA catalysts in catalytic decomposition of N2O. Journal of Catalysis, 2020, 392, 322-335.	3.1	27
57	Performance and Mechanism of Photocatalytic Toluene Degradation and Catalyst Regeneration by Thermal/UV Treatment. Environmental Science & Technology, 2020, 54, 14465-14473.	4.6	76
58	Roles of Oxygen Vacancies in the Bulk and Surface of CeO ₂ for Toluene Catalytic Combustion. Environmental Science & Technology, 2020, 54, 12684-12692.	4.6	231
59	New Insight into the In Situ SO2 Poisoning Mechanism over Cu-SSZ-13 for the Selective Catalytic Reduction of NOx with NH3. Catalysts, 2020, 10, 1391.	1.6	17
60	Quantitative Cu Counting Methodologies for Cu/SSZ-13 Selective Catalytic Reduction Catalysts by Electron Paramagnetic Resonance Spectroscopy. Journal of Physical Chemistry C, 2020, 124, 28061-28073.	1.5	20
61	The deactivation mechanism of toluene on MnOx-CeO2 SCR catalyst. Applied Catalysis B: Environmental, 2020, 277, 119257.	10.8	86
62	Rational tuning towards A/B-sites double-occupying cobalt on tri-metallic spinel: Insights into its catalytic activity on toluene catalytic oxidation. Chemical Engineering Journal, 2020, 399, 125792.	6.6	30
63	Controllable redox-induced in-situ growth of MnO2 over Mn2O3 for toluene oxidation: Active heterostructure interfaces. Applied Catalysis B: Environmental, 2020, 278, 119279.	10.8	131
64	Probing Active-Site Relocation in Cu/SSZ-13 SCR Catalysts during Hydrothermal Aging by In Situ EPR Spectroscopy, Kinetics Studies, and DFT Calculations. ACS Catalysis, 2020, 10, 9410-9419.	5.5	64
65	Severe deactivation and artificial enrichment of thallium on commercial SCR catalysts installed in cement kiln. Applied Catalysis B: Environmental, 2020, 277, 119194.	10.8	20
66	Sn-doped rutile TiO2 for vanadyl catalysts: Improvements on activity and stability in SCR reaction. Applied Catalysis B: Environmental, 2020, 269, 118797.	10.8	57
67	The poisoning mechanism of gaseous HCl on low-temperature SCR catalysts: MnO â^'CeO2 as an example. Applied Catalysis B: Environmental, 2020, 267, 118668.	10.8	82
68	The role of the Cu dopant on a Mn3O4 spinel SCR catalyst: Improvement of low-temperature activity and sulfur resistance. Chemical Engineering Journal, 2020, 387, 124090.	6.6	124
69	Distinctive Bimetallic Oxides for Enhanced Catalytic Toluene Combustion: Insights into the Tunable Fabrication of Mnâ~'Ce Hollow Structure. ChemCatChem, 2020, 12, 2872-2879.	1.8	27
70	Low content of CoOx supported on nanocrystalline CeO2 for toluene combustion: The importance of interfaces between active sites and supports. Applied Catalysis B: Environmental, 2019, 240, 329-336.	10.8	124
71	NH3-SCR performance of WO3 blanketed CeO2 with different morphology: Balance of surface reducibility and acidity. Catalysis Today, 2019, 332, 42-48.	2.2	79
72	lron tungsten mixed composite as a robust oxygen evolution electrocatalyst. Chemical Communications, 2019, 55, 10944-10947.	2.2	28

#	Article	IF	CITATIONS
73	Balance between Reducibility and N ₂ O Adsorption Capacity for the N ₂ O Decomposition: Cu _{<i>x</i>} Co _{<i>y</i>} Catalysts as an Example. Environmental Science & Technology, 2019, 53, 10379-10386.	4.6	36
74	The Roles of Various Plasma Active Species in Toluene Degradation by Non-thermal Plasma and Plasma Catalysis. Plasma Chemistry and Plasma Processing, 2019, 39, 1469-1482.	1.1	17
75	The synergistic mechanism of NO _x and chlorobenzene degradation in municipal solid waste incinerators. Catalysis Science and Technology, 2019, 9, 4286-4292.	2.1	39
76	Comparison of NH3-SCO performance over CuOx/H-SSZ-13 and CuOx/H-SAPO-34 catalysts. Applied Catalysis A: General, 2019, 585, 117119.	2.2	17
77	Enhanced low-temperature activity of LaMnO3 for toluene oxidation: The effect of treatment with an acidic KMnO4. Chemical Engineering Journal, 2019, 366, 92-99.	6.6	112
78	Application of Nanotechnology in Pollution Control of NOx From Stationary Sources. , 2019, , 179-211.		2
79	Vanadium-density-dependent thermal decomposition of NH ₄ HSO ₄ on V ₂ O ₅ /TiO ₂ SCR catalysts. Catalysis Science and Technology, 2019, 9, 3779-3787.	2.1	31
80	Deactivation of Pt-Au/TiO2-CeO2 catalyst for co-oxidation of HCHO, H2 and CO at room temperature: Degradations of active sites and mutual influence between reactants. Applied Catalysis A: General, 2019, 582, 117116.	2.2	22
81	Insights over Titanium Modified FeMgOx Catalysts for Selective Catalytic Reduction of NOx with NH3: Influence of Precursors and Crystalline Structures. Catalysts, 2019, 9, 560.	1.6	9
82	Using Transient FTIR Spectroscopy to Probe Active Sites and Reaction Intermediates for Selective Catalytic Reduction of NO on Cu/SSZ-13 Catalysts. ACS Catalysis, 2019, 9, 6137-6145.	5.5	105
83	Hollow-Structural Ag/Co ₃ O ₄ Nanocatalyst for CO Oxidation: Interfacial Synergistic Effect. ACS Applied Nano Materials, 2019, 2, 3480-3489.	2.4	60
84	Modified Silica Adsorbents for Toluene Adsorption under Dry and Humid Conditions: Impacts of Pore Size and Surface Chemistry. Langmuir, 2019, 35, 8927-8934.	1.6	24
85	Effect of Fe precursors on the catalytic activity of Fe/SAPO-34 catalysts for N2O decomposition. Catalysis Communications, 2019, 128, 105706.	1.6	16
86	Deactivation Mechanism of Multipoisons in Cement Furnace Flue Gas on Selective Catalytic Reduction Catalysts. Environmental Science & Technology, 2019, 53, 6937-6944.	4.6	75
87	Fe-Doped α-MnO ₂ nanorods for the catalytic removal of NO _x and chlorobenzene: the relationship between lattice distortion and catalytic redox properties. Physical Chemistry Chemical Physics, 2019, 21, 25880-25888.	1.3	39
88	Investigation on removal of NO and HgO with different Cu species in Cu-SAPO-34 zeolites. Catalysis Communications, 2019, 119, 91-95.	1.6	17
89	Highly selective α-Mn2O3 catalyst for cGPF soot oxidation: Surface activated oxygen enhancement via selective dissolution. Chemical Engineering Journal, 2019, 364, 448-451.	6.6	35
90	Effects of dietary vitamin C and vitamin E on the growth, antioxidant defence and digestive enzyme activities of juvenile discus fish (<i>Symphysodon haraldi</i>). Aquaculture Nutrition, 2019, 25, 176-183.	1.1	31

#	Article	IF	CITATIONS
91	The promotion effect of ceria on high vanadia loading NH3-SCR catalysts. Catalysis Communications, 2019, 121, 84-88.	1.6	16
92	Selective Catalytic Reduction of NO _{<i>x</i>} with Ammonia over Copper Ion Exchanged SAPOâ€47 Zeolites in a Wide Temperature Range. ChemCatChem, 2018, 10, 2481-2487.	1.8	10
93	Non-thermal plasma catalysis for chlorobenzene removal over CoMn/TiO2 and CeMn/TiO2: Synergistic effect of chemical catalysis and dielectric constant. Chemical Engineering Journal, 2018, 347, 447-454.	6.6	76
94	Preparation of <i>γ</i> â€Fe ₂ O ₃ Catalysts and their deNO <i>_x</i> Performance: Effects of Precipitation Conditions. Chemical Engineering and Technology, 2018, 41, 1019-1026.	0.9	2
95	Interaction of phosphorus with a FeTiOx catalyst for selective catalytic reduction of NOx with NH3: Influence on surface acidity and SCR mechanism. Chemical Engineering Journal, 2018, 347, 173-183.	6.6	72
96	Carbon Dioxide Promotes Dehydrogenation in the Equimolar C 2 H 2 O 2 Reaction to Synthesize Carbon Nanotubes. Small, 2018, 14, 1703482.	5.2	8
97	NO _{<i>x</i>} Removal over V ₂ O ₅ /WO ₃ –TiO ₂ Prepared by a Grinding Method: Influence of the Precursor on Vanadium Dispersion. Industrial & Engineering Chemistry Research, 2018. 57. 150-157.	1.8	32
98	Dechlorination of chlorobenzene on vanadium-based catalysts for low-temperature SCR. Chemical Communications, 2018, 54, 2032-2035.	2.2	63
99	De-reducibility mechanism of titanium on maghemite catalysts for the SCR reaction: An in situ DRIFTS and quantitative kinetics study. Applied Catalysis B: Environmental, 2018, 221, 556-564.	10.8	116
100	Studies on toluene adsorption performance and hydrophobic property in phenyl functionalized KIT-6. Chemical Engineering Journal, 2018, 334, 191-197.	6.6	56
101	Novel nanowire self-assembled hierarchical CeO2 microspheres for low temperature toluene catalytic combustion. Chemical Engineering Journal, 2018, 331, 425-434.	6.6	135
102	Promotion Effect of Gaâ^'Co Spinel Derived from Layered Double Hydroxides for Toluene Oxidation. ChemCatChem, 2018, 10, 4838-4843.	1.8	30
103	Promotion of H ₃ PW ₁₂ O ₄₀ Grafting on NO _{<i>x</i>} Abatement over γ-Fe ₂ O ₃ : Performance and Reaction Mechanism. Industrial & Engineering Chemistry Research, 2018, 57, 13661-13670.	1.8	22
104	Facile surface improvement method for LaCoO ₃ for toluene oxidation. Catalysis Science and Technology, 2018, 8, 3166-3173.	2.1	111
105	Different exposed facets VO /CeO2 catalysts for the selective catalytic reduction of NO with NH3. Chemical Engineering Journal, 2018, 349, 184-191.	6.6	86
106	Engineering surface functional groups on mesoporous silica: towards a humidity-resistant hydrophobic adsorbent. Journal of Materials Chemistry A, 2018, 6, 13769-13777.	5.2	39
107	A dual-functional MnO2/La0.6Sr0.4MnO3 composite catalyst: high-efficiency for elemental mercury oxidation in flue gas. Catalysis Communications, 2018, 112, 43-48.	1.6	4
108	MnO -CeO2 catalysts for effective NO reduction in the presence of chlorobenzene. Catalysis Communications, 2018, 117, 1-4.	1.6	49

#	Article	IF	CITATIONS
109	Synergistic Promotion Effect between NO _{<i>x</i>} and Chlorobenzene Removal on MnO _{<i>x</i>} –CeO ₂ Catalyst. ACS Applied Materials & Interfaces, 2018, 10, 30426-30432.	4.0	74
110	Performance of Modified La _{<i>x</i>} Sr _{1–<i>x</i>} MnO ₃ Perovskite Catalysts for NH ₃ Oxidation: TPD, DFT, and Kinetic Studies. Environmental Science & Technology, 2018, 52, 7443-7449.	4.6	67
111	Extraordinary Deactivation Offset Effect of Arsenic and Calcium on CeO ₂ –WO ₃ SCR Catalysts. Environmental Science & Technology, 2018, 52, 8578-8587.	4.6	73
112	Templateâ€free Scalable Synthesis of Flowerâ€like Co _{3â€<i>x</i>} Mn _{<i>x</i>} O ₄ Spinel Catalysts for Toluene Oxidation. ChemCatChem, 2018, 10, 3429-3434.	1.8	125
113	Influence of sulfation on CeO2-ZrO2 catalysts for NO reduction with NH3. Chinese Journal of Catalysis, 2017, 38, 160-167.	6.9	12
114	Impacts of Pb and SO ₂ Poisoning on CeO ₂ –WO ₃ /TiO ₂ –SiO ₂ SCR Catalyst. Environmental Science & Technology, 2017, 51, 11943-11949.	4.6	90
115	The relationship between surface open cells of α-MnO ₂ and CO oxidation ability from a surface point of view. Journal of Materials Chemistry A, 2017, 5, 20911-20921.	5.2	38
116	A neutral and coordination regeneration method of Ca-poisoned V2O5-WO3/TiO2 SCR catalyst. Catalysis Communications, 2017, 100, 112-116.	1.6	30
117	Novel W-modified SnMnCeO catalyst for the selective catalytic reduction of NO with NH3. Catalysis Communications, 2017, 100, 117-120.	1.6	19
118	Surface Tuning of La _{0.5} Sr _{0.5} CoO ₃ Perovskite Catalysts by Acetic Acid for NO _{<i>x</i>} Storage and Reduction. Environmental Science & Technology, 2016, 50, 6442-6448.	4.6	108
119	Investigation of the Poisoning Mechanism of Lead on the CeO ₂ —WO ₃ Catalyst for the NH ₃ –SCR Reaction via in Situ IR and Raman Spectroscopy Measurement. Environmental Science & Technology, 2016, 50, 9576-9582.	4.6	106
120	Comparison of the Structures and Mechanism of Arsenic Deactivation of CeO ₂ –MoO ₃ and CeO ₂ –WO ₃ SCR Catalysts. Journal of Physical Chemistry C, 2016, 120, 18005-18014.	1.5	64
121	NH3 selective catalytic reduction of NO: A large surface TiO2 support and its promotion of V2O5 dispersion on the prepared catalyst. Chinese Journal of Catalysis, 2016, 37, 878-887.	6.9	20
122	Chemical poison and regeneration of SCR catalysts for NO x removal from stationary sources. Frontiers of Environmental Science and Engineering, 2016, 10, 413-427.	3.3	100
123	Perfluorooctanoic Acid Degradation Using UV–Persulfate Process: Modeling of the Degradation and Chlorate Formation. Environmental Science & Technology, 2016, 50, 772-781.	4.6	294
124	Mechanism of arsenic poisoning on SCR catalyst of CeW/Ti and its novel efficient regeneration method with hydrogen. Applied Catalysis B: Environmental, 2016, 184, 246-257.	10.8	149
125	Identification of the reaction pathway and reactive species for the selective catalytic reduction of NO with NH ₃ over cerium–niobium oxide catalysts. Catalysis Science and Technology, 2016, 6, 2136-2142.	2.1	49
126	Comparison of MoO3 and WO3 on arsenic poisoning V2O5/TiO2 catalyst: DRIFTS and DFT study. Applied Catalysis B: Environmental, 2016, 181, 692-698.	10.8	117

#	Article	IF	CITATIONS
127	Selective Dissolution of A‧ite Cations in ABO ₃ Perovskites: A New Path to Highâ€Performance Catalysts. Angewandte Chemie - International Edition, 2015, 54, 7954-7957.	7.2	180
128	Selective Dissolution of A‧ite Cations in ABO ₃ Perovskites: A New Path to Highâ€Performance Catalysts. Angewandte Chemie, 2015, 127, 8065-8068.	1.6	58
129	Lean NO –SnO2–CeO2 catalyst at low temperatures. Catalysis Today, 2015, 258, 556-563.	2.2	6
130	Ceria promotion on the potassium resistance of MnOx/TiO2 SCR catalysts: An experimental and DFT study. Chemical Engineering Journal, 2015, 269, 44-50.	6.6	92
131	Selective catalytic reduction of NO with NH ₃ over novel iron–tungsten mixed oxide catalyst in a broad temperature range. Catalysis Science and Technology, 2015, 5, 4556-4564.	2.1	65
132	The promotional effect of MoO3 doped V2O5/TiO2 for chlorobenzene oxidation. Catalysis Communications, 2015, 69, 161-164.	1.6	34
133	The outstanding performance of LDH-derived mixed oxide Mn/CoAlO _x for Hg ⁰ oxidation. Catalysis Science and Technology, 2015, 5, 3536-3544.	2.1	27
134	Experimental and DFT studies on Sr-doped LaMnO ₃ catalysts for NO _x storage and reduction. Catalysis Science and Technology, 2015, 5, 2478-2485.	2.1	48
135	Fabrication and Electrochemical Treatment Application of an Al-Doped PbO ₂ Electrode with High Oxidation Capability, Oxygen Evolution Potential and Reusability. Journal of the Electrochemical Society, 2015, 162, E258-E262.	1.3	30
136	Ultra hydrothermal stability of CeO2-WO3/TiO2 for NH3-SCR of NO compared to traditional V2O5-WO3/TiO2 catalyst. Catalysis Today, 2015, 258, 11-16.	2.2	61
137	Regeneration of Commercial SCR Catalysts: Probing the Existing Forms of Arsenic Oxide. Environmental Science & Technology, 2015, 49, 9971-9978.	4.6	89
138	Correlation of the changes in the framework and active Cu sites for typical Cu/CHA zeolites (SSZ-13) Tj ETQq0 0	0 rgBT /Ov 1.3	verlock 10 Tf
139	A high-efficiency γ-MnO ₂ -like catalyst in toluene combustion. Chemical Communications, 2015, 51, 14977-14980.	2.2	153
140	Removal of Antimonite (Sb(III)) and Antimonate (Sb(V)) from Aqueous Solution Using Carbon Nanofibers That Are Decorated with Zirconium Oxide (ZrO ₂). Environmental Science & Technology, 2015, 49, 11115-11124.	4.6	233
141	Reaction Pathway Investigation on the Selective Catalytic Reduction of NO with NH ₃ over Cu/SSZ-13 at Low Temperatures. Environmental Science & amp; Technology, 2015, 49, 467-473.	4.6	87
142	Synthesis, characterization, and catalytic evaluation of Co 3 O 4 /γ-Al 2 O 3 as methane combustion catalysts: Significance of Co species and the redox cycle. Applied Catalysis B: Environmental, 2015, 168-169, 42-50.	10.8	90
143	Deactivation and regeneration of a commercial SCR catalyst: Comparison with alkali metals and arsenic. Applied Catalysis B: Environmental, 2015, 168-169, 195-202.	10.8	180

An experimental and DFT study of the adsorption and oxidation of NH3 on a CeO2 catalyst modified by 2.2 51 Fe, Mn, La and Y. Catalysis Today, 2015, 242, 300-307.

#	Article	IF	CITATIONS
145	Effects of noble metals doped on mesoporous <scp>LaAlNi</scp> mixed oxide catalyst and identification of carbon deposit for reforming <scp>CH₄</scp> with <scp>CO₂</scp> . Journal of Chemical Technology and Biotechnology, 2014, 89, 372-381.	1.6	51
146	Structure–activity relationship of VOx/CeO2 nanorod for NO removal with ammonia. Applied Catalysis B: Environmental, 2014, 144, 538-546.	10.8	144
147	Investigation on a novel CaO–Y2O3 sorbent for efficient CO2 mitigation. Chemical Engineering Journal, 2014, 243, 297-304.	6.6	103
148	Insight into Deactivation of Commercial SCR Catalyst by Arsenic: An Experiment and DFT Study. Environmental Science & Technology, 2014, 48, 13895-13900.	4.6	98
149	Deactivation Mechanism of Potassium on the V ₂ O ₅ /CeO ₂ Catalysts for SCR Reaction: Acidity, Reducibility and Adsorbed-NO _{<i>x</i>} . Environmental Science & Technology, 2014, 48, 4515-4520.	4.6	137
150	Mechanism of N ₂ O Formation during the Low-Temperature Selective Catalytic Reduction of NO with NH ₃ over Mn–Fe Spinel. Environmental Science & Technology, 2014, 48, 10354-10362.	4.6	225
151	Characterization of CeO2–WO3 catalysts prepared by different methods for selective catalytic reduction of NO with NH3. Catalysis Communications, 2013, 40, 145-148.	1.6	61
152	Identification of the active sites on CeO2–WO3 catalysts for SCR of NOx with NH3: An in situ IR and Raman spectroscopy study. Applied Catalysis B: Environmental, 2013, 140-141, 483-492.	10.8	295
153	Dispersion of tungsten oxide on SCR performance of V2O5WO3/TiO2: Acidity, surface species and catalytic activity. Chemical Engineering Journal, 2013, 225, 520-527.	6.6	177
154	Low temperature complete combustion of methane over cobalt chromium oxides catalysts. Catalysis Today, 2013, 201, 12-18.	2.2	100
155	Structural effects of iron spinel oxides doped with Mn, Co, Ni and Zn on selective catalytic reduction of NO with NH3. Journal of Molecular Catalysis A, 2013, 376, 13-21.	4.8	68
156	Dextrose-aided hydrothermal preparation with large surface area on 1D single-crystalline perovskite La0.5Sr0.5CoO3 nanowires without template: Highly catalytic activity for methane combustion. Journal of Molecular Catalysis A, 2013, 378, 299-306.	4.8	56
157	The effect of SiO2 on a novel CeO2–WO3/TiO2 catalyst for the selective catalytic reduction of NO with NH3. Applied Catalysis B: Environmental, 2013, 140-141, 276-282.	10.8	110
158	Ammonia adsorption on graphene and graphene oxide: a first-principles study. Frontiers of Environmental Science and Engineering, 2013, 7, 403-411.	3.3	111
159	Novel effect of SO2 on the SCR reaction over CeO2: Mechanism and significance. Applied Catalysis B: Environmental, 2013, 136-137, 19-28.	10.8	312
160	The relationship between structure and activity of MoO3–CeO2 catalysts for NO removal: influences of acidity and reducibility. Chemical Communications, 2013, 49, 6215.	2.2	113
161	Comparison on the Performance of α-Fe2O3 and γ-Fe2O3 for Selective Catalytic Reduction of Nitrogen Oxides with Ammonia. Catalysis Letters, 2013, 143, 697-704.	1.4	101
162	Substitution of WO ₃ in V ₂ O ₅ /WO ₃ –TiO ₂ by Fe ₂ O ₃ for selective catalytic reduction of NO with NH3. Catalysis Science and Technology, 2013, 3, 161-168.	2.1	90

#	Article	IF	CITATIONS
163	Design Strategies for Development of SCR Catalyst: Improvement of Alkali Poisoning Resistance and Novel Regeneration Method. Environmental Science & Technology, 2012, 46, 12623-12629.	4.6	134
164	Alkali Metal Poisoning of a CeO ₂ –WO ₃ Catalyst Used in the Selective Catalytic Reduction of NO _{<i>x</i>} with NH ₃ : an Experimental and Theoretical Study. Environmental Science & Technology, 2012, 46, 2864-2869.	4.6	200
165	A novel magnetic Fe–Ti–V spinel catalyst for the selective catalytic reduction of NO with NH3 in a broad temperature range. Catalysis Science and Technology, 2012, 2, 915.	2.1	53
166	Manganese doped CeO2–WO3 catalysts for the selective catalytic reduction of NO with NH3: An experimental and theoretical study. Catalysis Communications, 2012, 19, 127-131.	1.6	55
167	Fe–Ti spinel for the selective catalytic reduction of NO with NH3: Mechanism and structure–activity relationship. Applied Catalysis B: Environmental, 2012, 117-118, 73-80.	10.8	178